

Electronic Supplementary Information

Persistent radical anion derived from a propeller-shaped perylene bisimide-carbazole pentad

Zhaolong Wang,^a Xinyu Gou,^a Gang Wang,^a Xingmao Chang,^a Ke Liu,^a Taihong Liu,^{*,a} Gang He,^b and Yu Fang^{*,a}

^a Key Laboratory of Applied Surface and Colloid Chemistry of Ministry of Education, School of Chemistry and Chemical Engineering, Shaanxi Normal University, Xi'an 710119, P. R. China

^b Frontier Institute of Science and Technology, Xi'an Jiaotong University, Xi'an 710054, P. R. China

*E-mails: yfang@snnu.edu.cn (Y. Fang), liuth121@snnu.edu.cn (T. Liu)

Table of Contents

| | |
|--|-----|
| 1. General experimental information..... | S3 |
| 2. Supplementary figures and tables..... | S4 |
| <i>References</i> | S18 |

1. General experimental information

Solvents and reagents: All the solvents and reagents with at least analytical grade were purchased from commercial sources (Adamas-beta) and used as received without further purification. Cobaltocene (CoCp_2) was handled and stored in a glovebox.

Instrumental methods: Single-crystal X-ray diffraction was obtained using a Bruker SMART APEX II single-crystal X-ray diffraction spectrometer. UV-Vis-NIR absorption spectra in solution were recorded on a Perkin-Elmer Lambd 1050 spectrophotometer at room temperature. Electron paramagnetic resonance (EPR) measurements were carried out at room temperature using a Bruker ELEXSYS E500 EPR spectrometer. All samples were reduced using CoCp_2 as the chemical reductant and loaded into 1.4 mm I.D. quartz tubes, which were sealed with epoxy resin in an argon-filled glovebox and used immediately after preparation. Scans were performed with magnetic field modulation amplitude of 0.1 G. The optical images depicted in the paper were recorded using a Canon 70D camera. The light irradiation tests were carried out by white light of a xenon lamp from Beijing Perfectlight Technology Co., Ltd.

Quantum chemical calculation: The geometry of radical anion of PBI-4Cz was optimized by using the broken symmetry and the calculation was carried out using the DFT method with UCAM-B3LYP employing the 6-31G(d) basis set for all atoms. The calculated results were processed by Multiwfn.¹⁻³

2. Supplementary figures and tables

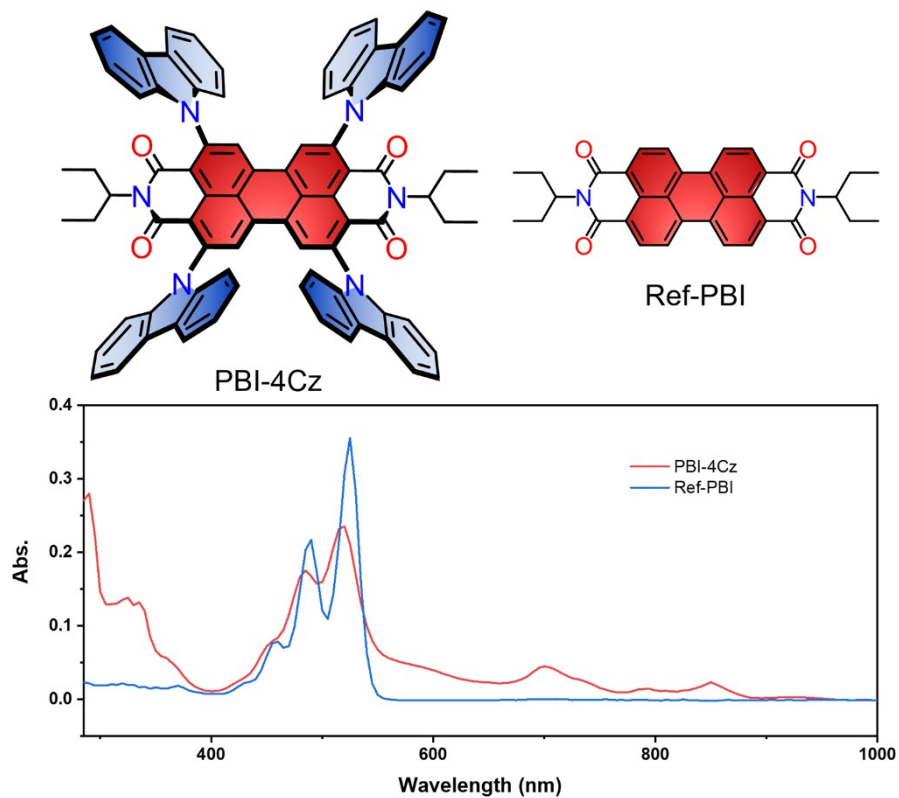


Figure S1. Chemical structures of PBI-4Cz and Ref-PBI and their UV-Vis-NIR absorption spectra in DMF.

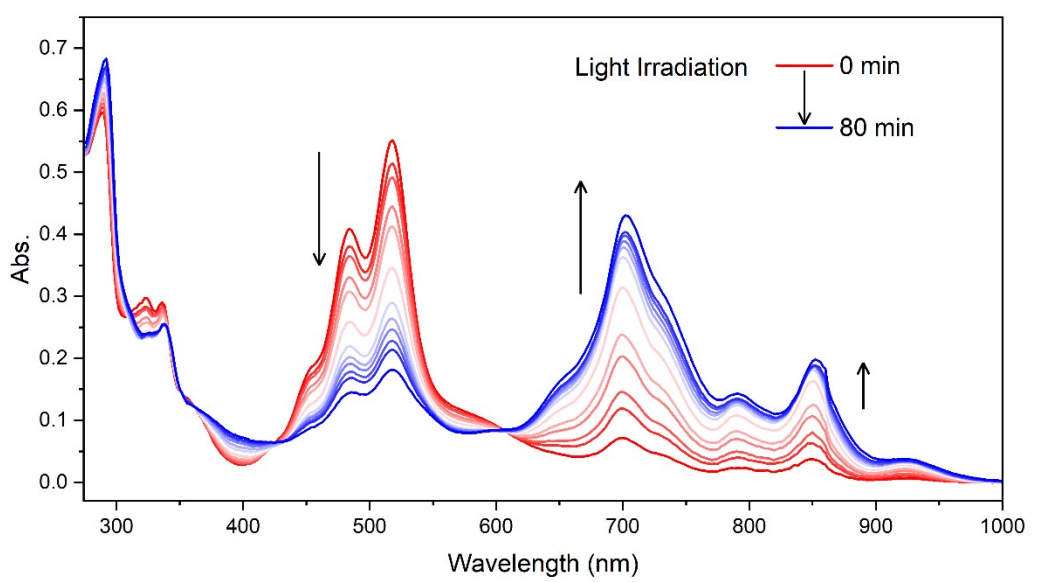


Figure S2. Changes in the UV-Vis-NIR absorption spectra of PBI-4Cz in DMF upon light irradiation ($C \sim 1.0 \times 10^{-5}$ mol/L).

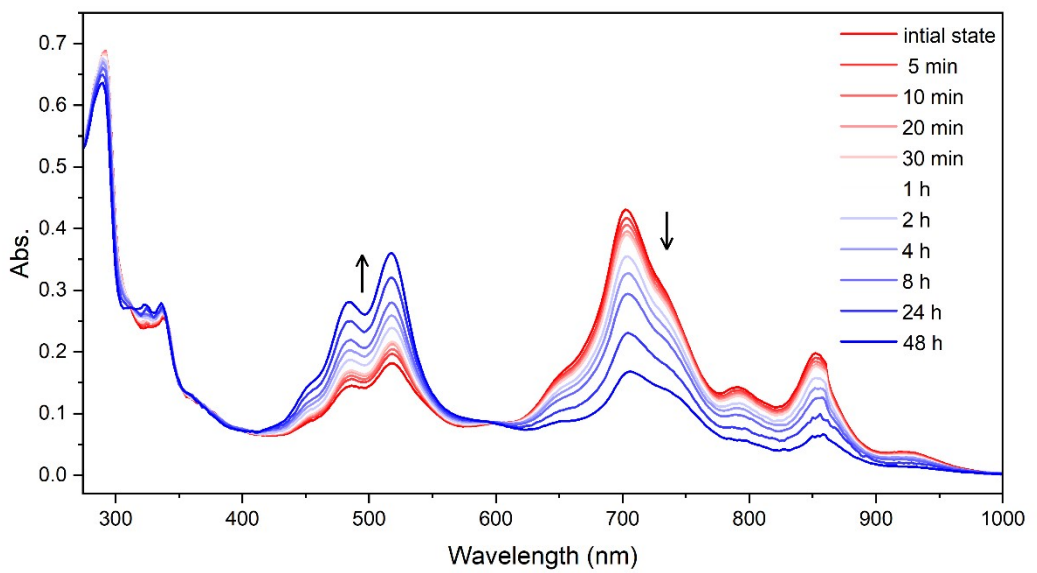


Figure S3. Time-dependent UV-Vis-NIR spectra of PBI-4Cz in DMF under dark condition ($C \sim 1.0 \times 10^{-5}$ mol/L).

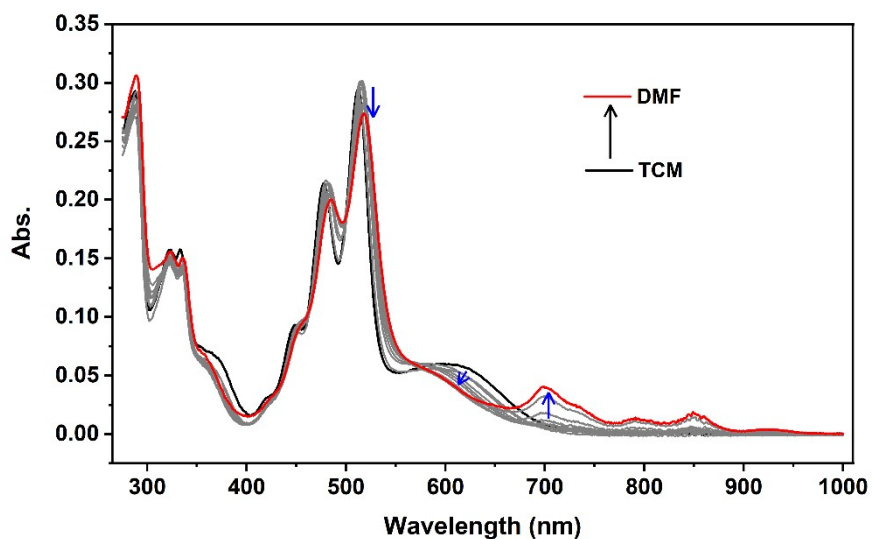


Figure S4. UV-Vis-NIR absorption spectra of PBI-4Cz in the binary mixture of DMF and chloroform ($C \sim 5.0 \times 10^{-6}$ mol/L, 298 K).

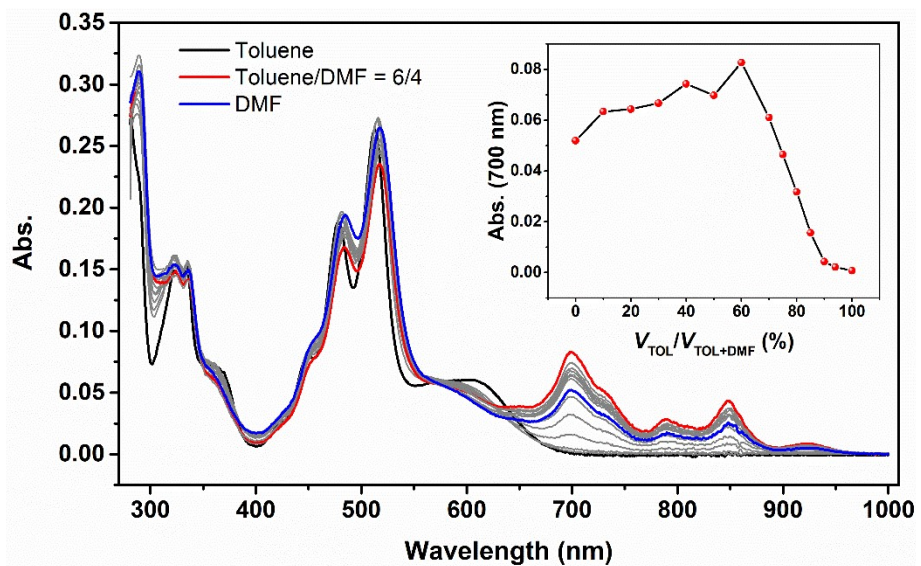


Figure S5. UV-Vis-NIR absorption spectra of PBI-4Cz in the binary mixture of DMF and toluene ($C \sim 5.0 \times 10^{-6}$ mol/L, 298 K). *Inset:* Plot of absorbance at 700 nm versus the content of toluene.

Table S1. Summarized electrochemical properties of PBI-4Cz and Ref-PBI.⁴

| Compound | $E_{\text{1st-red}}/\text{V}$ | $E_{\text{2nd-red}}/\text{V}$ | $E_{\text{LUMO}}/\text{eV}$ |
|----------|-------------------------------|-------------------------------|-----------------------------|
| PBI-4Cz | -0.87 | -1.20 | -3.93 |
| Ref-PBI | -1.10 | -1.30 | -3.70 |

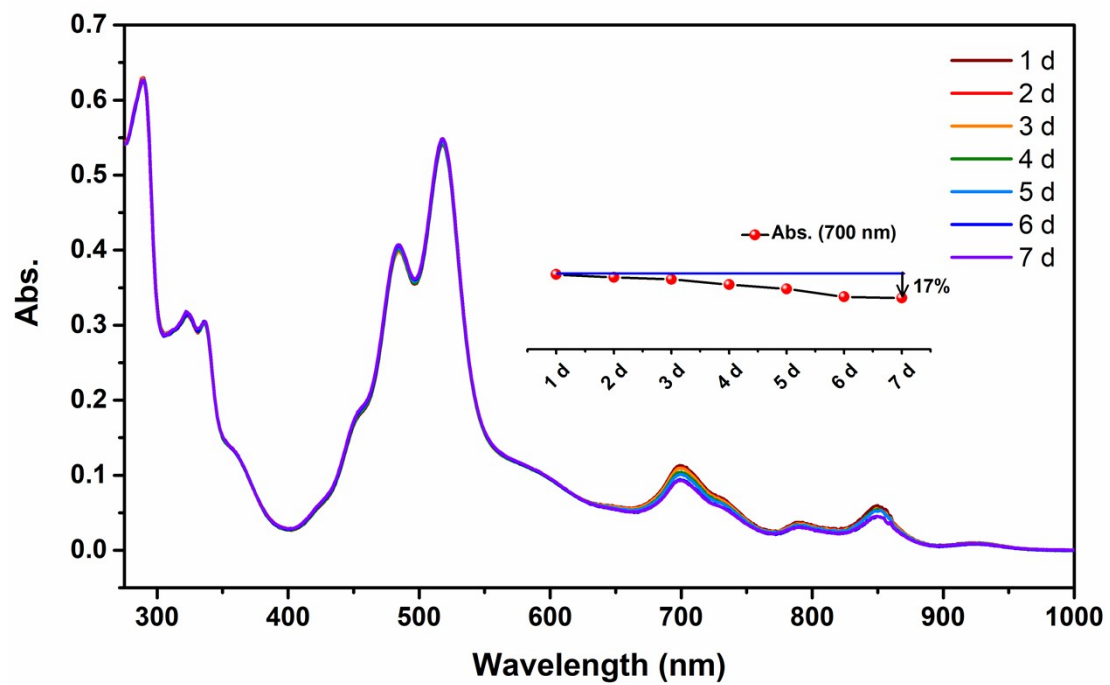


Figure S6. Time-dependent UV-Vis-NIR spectra of PBI-4Cz in DMF under ambient air ($C \sim 1.0 \times 10^{-5}$ mol/L, 298 K).

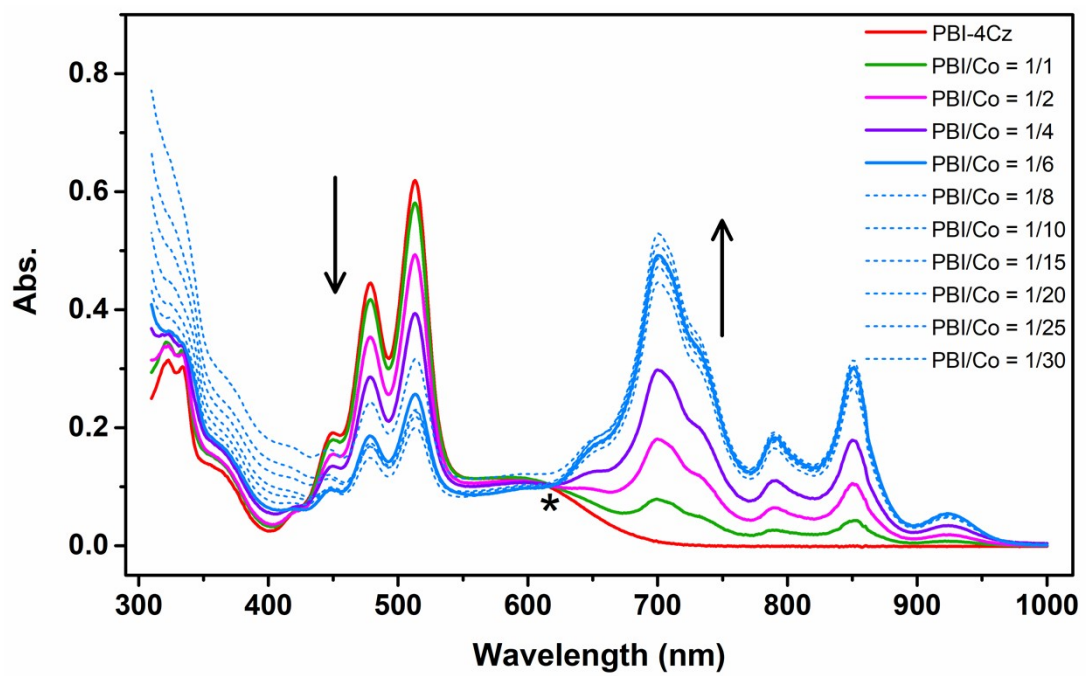


Figure S7. UV-Vis-NIR absorption spectra of PBI-4Cz in CH_2Cl_2 ($C \sim 1.0 \times 10^{-5}$ mol/L, 298 K) upon gradual addition of CoCp_2 .

Table S2. Crystal data and structure refinement for [PBI-4Cz]·(CoCp₂)₂

| | |
|-----------------------------------|---|
| Identification code | [PBI-4Cz]·(CoCp ₂) ₂ |
| Empirical formula | C ₁₀₅ H ₈₇ Co ₂ N ₇ O ₅ |
| Formula weight | 1644.67 |
| Temperature | 235(2) K |
| Wavelength | 1.34139 Å |
| Crystal system | Orthorhombic |
| Space group | P2 ₁ 2 ₁ 2 ₁ |
| Unit cell dimensions | a = 18.044(10) Å α = 90 ° b = 32.231(19) Å β = 90 ° c = 16.800(9) Å γ = 90 ° |
| Volume | 9770(10) Å ³ |
| Z | 4 |
| Density (calculated) | 1.118 mg/m ³ |
| Absorption coefficient | 2.129 mm ⁻¹ |
| F(000) | 3440 |
| Crystal size | 0.100 × 0.100 × 0.100 mm ³ |
| Theta range for data collection | 2.385 to 51.587 ° |
| Index ranges | -20≤h≤19, -32≤k≤37, -19≤l≤19 |
| Reflections collected | 71096 |
| Independent reflections | 15928 [R(int) = 0.2030] |
| Completeness to theta = 51.587 ° | 98.2 % |
| Absorption correction | Semi-empirical from equivalents |
| Max. and min. transmission | 0.7501 and 0.5565 |
| Refinement method | Full-matrix least-squares on F ² |
| Data/restraints/parameters | 15928/828/1042 |
| Goodness-of-fit on F ² | 0.901 |
| Final R indices [I>2sigma(I)] | R ₁ = 0.0911, wR ₂ = 0.2116 |
| R indices (all data) | R ₁ = 0.2599, wR ₂ = 0.2967 |
| Absolute structure parameter | 0.446(16) |
| Extinction coefficient | n/a |
| Largest diff. peak and hole | 0.220 and -0.254 e.Å ⁻³ |

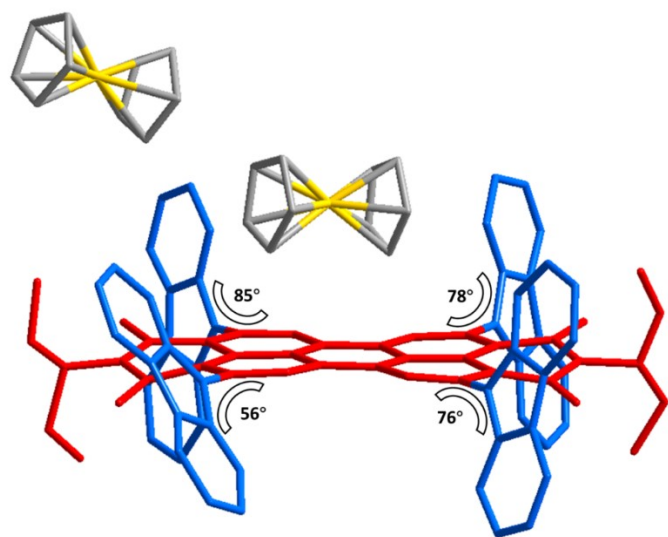


Figure S8. Dihedral angles between the plane of PBI and four carbazole moieties.

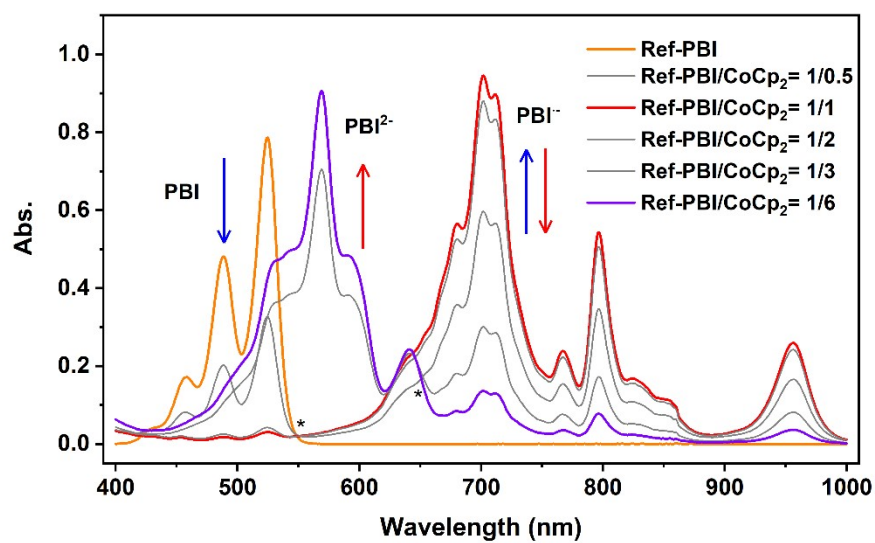


Figure S9. UV-Vis-NIR absorption spectra of Ref-PBI in DMF ($C \sim 1.0 \times 10^{-5}$ mol/L, 298 K) upon gradual addition of CoCp₂. Note: The isobestic points were marked with asterisk.

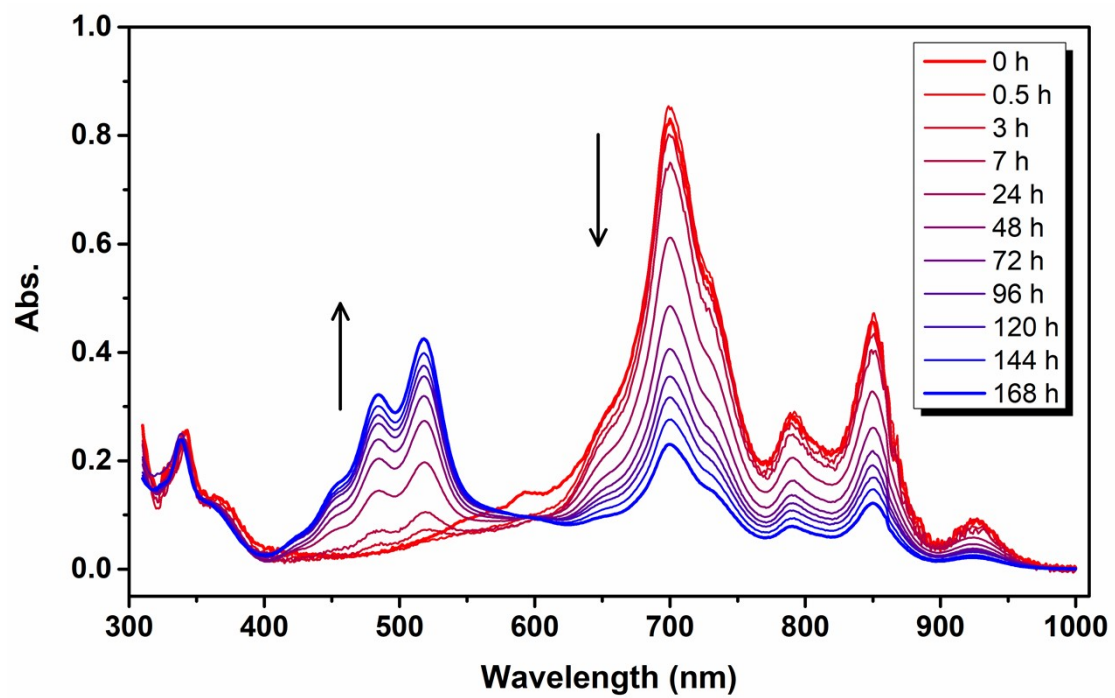


Figure S10. Time-dependent UV-Vis-NIR spectra of the fresh PBI⁻-4Cz in DMF under ambient air ($C \sim 1.0 \times 10^{-5}$ mol/L, 298 K). Note: The fresh PBI⁻-4Cz was obtained via chemically reduced method by CoCp₂.

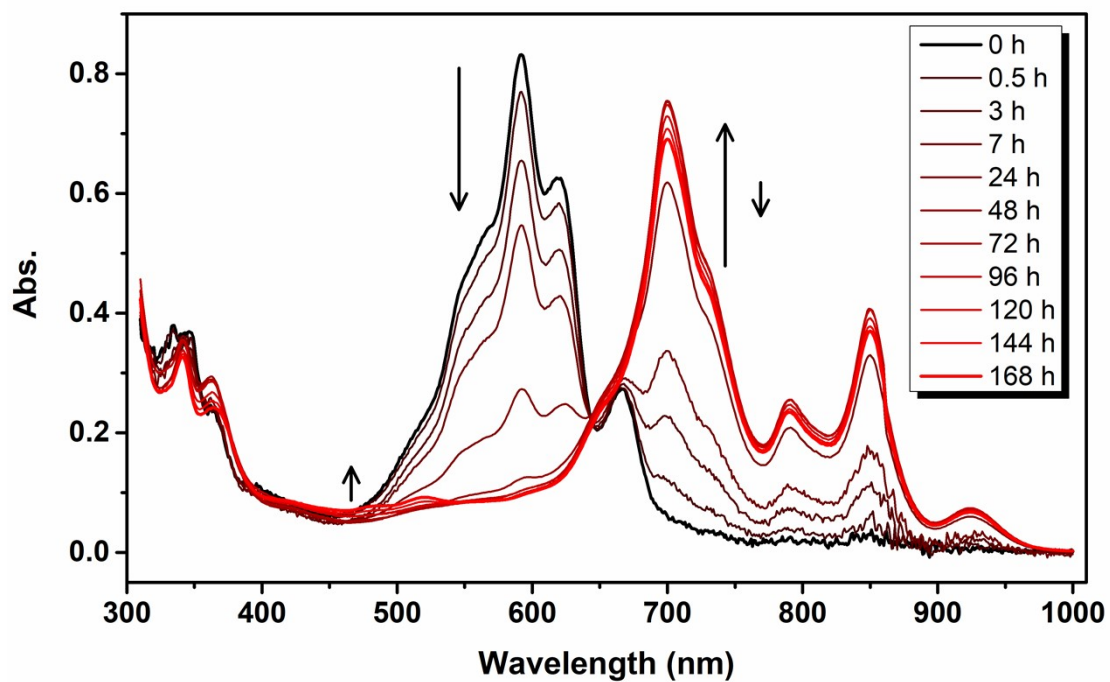


Figure S11. Time-dependent UV-Vis-NIR spectra of PBI²⁻-4Cz in DMF under ambient air ($C \sim 1.0 \times 10^{-5}$ mol/L, 298 K).

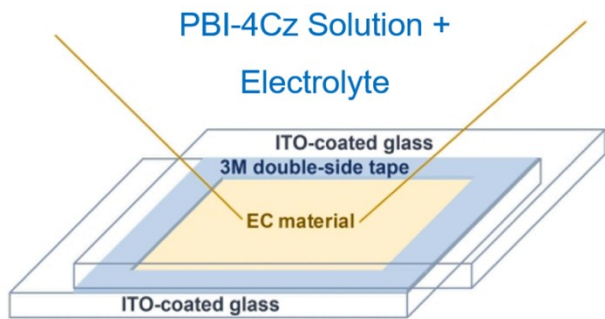


Figure S12. Schematic illustration of the PBI-4Cz solution-based electrochromic device.⁵

References

- [1] Frisch, M. J.; Trucks, G. W.; Schlegel, H. B.; Scuseria, G. E.; Robb, M. A.; Cheeseman, J. R.; Scalmani, G.; Barone, V.; Petersson, G. A.; Nakatsuji, H.; Li, X.; Caricato, M.; Marenich, A.; Bloino, J.; Janesko, B. G.; Gomperts, R.; Mennucci, B.; Hratchian, H. P.; Ortiz, J. V.; Izmaylov, A. F.; Sonnenberg, J. L.; Williams-Young, D.; Ding, F.; Lipparini, F.; Egidi, F.; Goings, J.; Peng, B.; Petrone, A.; Henderson, T.; Ranasinghe, D.; Zakrzewski, V. G.; Gao, J.; Rega, N.; Zheng, G.; Liang, W.; Hada, M.; Ehara, M.; Toyota, K.; Fukuda, R.; Hasegawa, J.; Ishida, M.; Nakajima, T.; Honda, Y.; Kitao, O.; Nakai, H.; Vreven, T.; Throssell, K.; Montgomery, J. A.; Jr.; Peralta, J. E.; Ogliaro, F.; Bearpark, M.; Heyd, J. J.; Brothers, E.; Kudin, K. N.; Staroverov, V. N.; Keith, T.; Kobayashi, R.; Normand, J.; Raghavachari, K.; Rendell, A.; Burant, J. C.; Iyengar, S. S.; Tomasi, J.; Cossi, M.; Millam, J. M.; Klene, M.; Adamo, C.; Cammi, R.; Ochterski, J. W.; Martin, R. L.; Morokuma, K.; Farkas, O.; Foresman, J. B.; Fox, D. J. *Gaussian 09, Version 9.0*, Gaussian, Inc., Wallingford, Connecticut, **2016**.
- [2] Dennington, R.; Keith, T.; Millam, J. *GaussView, Version 5*, Semichem Inc., Shawnee Mission, Kansas, **2009**.
- [3] Lu, T.; Chen, F. Multiwfn: A Multifunctional Wavefunction Analyzer. *J. Comput. Chem.* **2012**, *33*, 580-592.
- [4] Wang, Z.; Sun, Y.; Lin, S.; Wang, G.; Chang, X.; Gou, X.; Liu, T.; Jin, S.; He, G.; Wei, Y.-C.; Chou, P.-T.; Fang, Y. Orthogonal Carbazole-Perylene Bisimide Pentad: A Photoconversion-Tunable Photosensitizer with Diversified Excitation and Excited-State Relaxation Pathways. *Sci. China Chem.* **2021**, *64*, 2193-2202.
- [5] Song, R.; Li, G.; Zhang, Y.; Rao, B.; Xiong, S.; He, G. Novel Electrochromic Materials Based on Chalcogenoviologens for Smart Windows, E-Price Tag and Flexible Display with Improved Reversibility and Stability. *Chem. Eng. J.* **2021**, *422*, 130057.